Accelerating the convergence of the total energy evaluation in density functional theory calculations

Baojing Zhou and Yan Alexander Wang[a)]
Department of Chemistry, University of British Columbia, Vancouver, British Columbia V6T 1Z1, Canada

(Received 13 June 2007; accepted 9 November 2007; published online 25 February 2008)

A special feature of the Strutinsky shell correction method (SCM) [D. Ullmo *et al.*, Phys. Rev. B **63**, 125339 (2001)] and the recently proposed orbital-corrected orbital-free density functional theory (OO-DFT) [B. Zhou and Y. A. Wang, J. Chem. Phys. **124**, 081107 (2006)] is that the second-order corrections are incorporated in the total energy evaluation. In the SCM, the series expansion of the total electronic energy is essentially the Harris functional with its second-order correction. Unfortunately, a serious technical problem for the SCM is the lack of the exact Kohn-Sham (KS) density $\rho_{\mathrm{KS}}(\mathbf{r})$ required for the evaluation of the second-order correction. To overcome this obstacle, we design a scheme that utilizes the optimal density from a high-quality density mixing scheme to approximate $\rho_{\mathrm{KS}}(\mathbf{r})$. Recently, we proposed two total energy density functionals, i.e., the Zhou-Wang-λ (ZWλ) and the Wang-Zhou-α (WZα) functionals, for use in the OO-DFT method. If the two interpolation parameters, λ and α, are chosen to allow the second-order errors of the ZWλ and the WZα functionals to vanish, these two functionals reduce to the Hohenberg-Kohn-Sham functional with its second-order correction. Again, the optimal density from a high-quality density mixing scheme is used to approximate $\rho_{\mathrm{KS}}(\mathbf{r})$ in the evaluation of λ and α. This approach is tested in iterative KS-DFT calculations on systems with different chemical environments and can also be generalized for use in other iterative first-principles quantum chemistry methods. © *2008 American Institute of Physics*. [DOI: 10.1063/1.2821101]

I. INTRODUCTION

Density functional theory (DFT),[1,2] one of the most widely used first-principles quantum mechanics methods, provides a rigorous approach to treat the many-body problem of N interacting electrons. Currently, its widely used implementation is attributed to Kohn and Sham[3] (KS) and plays a vital role in understanding the properties of matter. In KS-DFT, one solves the following KS equations (in Hartree atomic units):

$$\left(-\tfrac{1}{2}\nabla^2 + v_{\mathrm{eff}}^{\mathrm{KS}}[\rho](\mathbf{r})\right)\phi_i(\mathbf{r}) = \epsilon_i\phi_i(\mathbf{r}), \tag{1}$$

where ϵ_i is the eigenvalue of the ith orbital, ϕ_i, and the KS effective potential, $v_{\mathrm{eff}}^{\mathrm{KS}}[\rho](\mathbf{r})$, contains the Hartree, exchange-correlation (XC), and ion-electron potentials,

$$\begin{aligned} v_{\mathrm{eff}}^{\mathrm{KS}}[\rho](\mathbf{r}) &= \frac{\delta E_{\mathrm{H}}[\rho]}{\delta\rho(\mathbf{r})} + \frac{\delta E_{\mathrm{xc}}[\rho]}{\delta\rho(\mathbf{r})} + v_{\mathrm{ne}}(\mathbf{r}) \\ &= v_{\mathrm{H}}[\rho](\mathbf{r}) + v_{\mathrm{xc}}[\rho](\mathbf{r}) + v_{\mathrm{ne}}(\mathbf{r}). \end{aligned} \tag{2}$$

With an iterative procedure,[4] each iteration of the KS-DFT calculation has two distinct steps. First, one solves Eq. (1) for ϵ_i and ϕ_i, with the KS effective potential, $v_{\mathrm{eff}}^{\mathrm{KS}}[\rho_{\mathrm{in}}](\mathbf{r})$, constructed from some fixed input density $\rho_{\mathrm{in}}(\mathbf{r})$. The output density is generated via

$$\rho_{\mathrm{out}}(\mathbf{r}) = \sum_i f_i|\phi_i(\mathbf{r})|^2, \tag{3}$$

where f_i is the occupation number of ϕ_i. Second, some density mixing scheme[4–6] is employed (in reciprocal space) to generate the optimal input density ρ_{in}^{i+1}, for the next iteration,

$$\rho_{\mathrm{in}}^{i+1} = \rho_{\mathrm{in}}^{i} + \mathbf{G}R[\rho_{\mathrm{in}}^{i}], \tag{4}$$

where $\mathbf{G}$ is the preconditioning matrix to reduce the density residual $R[\rho_{\mathrm{in}}]$,

$$R[\rho_{\mathrm{in}}] = \rho_{\mathrm{out}} - \rho_{\mathrm{in}}. \tag{5}$$

Note that the specific form of the $\mathbf{G}$ matrix depends on the density mixing scheme employed.[4] At each iteration, the total electronic energy is usually evaluated via the Hohenberg-Kohn-Sham (HKS) functional,[7]

$$\begin{aligned} E^{\mathrm{HKS}}[\rho_{\mathrm{in}},\rho_{\mathrm{out}}] &= \sum_i f_i\epsilon_i - \langle\rho_{\mathrm{out}}(\mathbf{r})\{v_{\mathrm{H}}[\rho_{\mathrm{in}}](\mathbf{r}) + v_{\mathrm{xc}}[\rho_{\mathrm{in}}](\mathbf{r})\}\rangle \\ &\quad + E_{\mathrm{H}}[\rho_{\mathrm{out}}] + E_{\mathrm{xc}}[\rho_{\mathrm{out}}], \end{aligned} \tag{6}$$

which always produces an upper bound to the exact total KS energy E^{KS}. The above process repeats itself until $R[\rho_{\mathrm{in}}]=0$ or the self-consistency is achieved: $\rho_{\mathrm{out}}(\mathbf{r})$ converges to the exact KS density $\rho_{\mathrm{KS}}(\mathbf{r})$ and E^{HKS} becomes identical to E^{KS},

$$\begin{aligned} E^{\mathrm{KS}}[\rho_{\mathrm{KS}}] &= \sum_i f_i\left\langle\phi_i^{\mathrm{KS}}\left|-\tfrac{1}{2}\nabla^2\right|\phi_i^{\mathrm{KS}}\right\rangle \\ &\quad + E_{\mathrm{H}}[\rho_{\mathrm{KS}}] + E_{\mathrm{xc}}[\rho_{\mathrm{KS}}] + \langle\rho_{\mathrm{KS}}(\mathbf{r})v_{\mathrm{ne}}(\mathbf{r})\rangle, \end{aligned} \tag{7}$$

where $\phi_i^{\mathrm{KS}}(\mathbf{r})$ is the ith converged KS orbital.

a)Author to whom correspondence should be addressed. Electronic mail: yawang@chem.ubc.ca.

Despite its great success, KS-DFT methods are still confronted with difficulties in its large-scale applications.[8] In the conventional KS-DFT method, the cost of each iteration scales as $\mathcal{O}(N^3)$ due to the orbital orthonormalization. Besides, many iterations are needed to achieve full self-consistency even with a high-quality density mixing scheme. With the development of massively parallel[9] and linear scaling[8] algorithms, it is feasible for KS-DFT to study systems of more than 1000 atoms.[9,10] Because of the computational cost of the conventional KS-DFT, the majority of KS-DFT calculations are still confined to systems fewer than 1000 atoms. On the other hand, in the original implementation of DFT, i.e., orbital-free (OF) DFT, one-electron orbitals are completely eliminated and the electron density is utilized as the sole variable.[11] Implemented with plane-wave basis set and modern fast Fourier transform technique,[12] OF-DFT has acquired quasilinear scaling with the computational cost of $\mathcal{O}(N \ln N)$.[13] With the aid of a fast Poisson solver, OF-DFT can achieve linear scaling in real space.[14] However, OF-DFT calculations have not attained high accuracy consistently, mainly due to the lack of an accurate kinetic energy density functional (KEDF).[13]

The Strutinsky shell correction method[15–18] (SCM) and the recently proposed orbital-corrected OF-DFT (OO-DFT) (Refs. 18–20) represent efforts to retain the merits of both KS-DFT and OF-DFT and avoid their drawbacks. In OO-DFT, it was further realized that more accurate nonlocal pseudopotentials[21] (NLPSs) can also be used to treat the valence-core interaction and the drawback of local pseudopotentials[22] (LPSs) required by OF-DFT is eliminated.[18–20] The efficiency of both approaches relies on two aspects: (i) improving the accuracy of OF-DFT so that high-quality input density can be obtained for the subsequent KS-DFT calculations and (ii) designing total energy density functionals that can achieve fast convergence. In this work, we focus on the second problem.

II. TOTAL ENERGY EVALUATION

Apart from the HKS functional, another widely used total energy density functional in KS-DFT was proposed by Harris based on perturbation theory,[23]

$$E^{\mathrm{Harris}}[\rho_{\mathrm{in}},\rho_{\mathrm{out}}] = \sum_i f_i \epsilon_i - E_{\mathrm{H}}[\rho_{\mathrm{in}}] + E_{\mathrm{xc}}[\rho_{\mathrm{in}}] - \langle \rho_{\mathrm{in}}(\mathbf{r}) v_{\mathrm{xc}}[\rho_{\mathrm{in}}](\mathbf{r})\rangle, \tag{8}$$

which sometimes predicts the total energy accurately even when the density residual $R[\rho_{\mathrm{in}}]$ is still big. However, the Harris functional is not necessarily more accurate than the HKS functional and is neither an upper bound nor a lower bound of E^{KS}.[24–26]

In 1990, Finnis derived the second-order errors in the HKS and the Harris functionals,[24]

$$E^{\mathrm{HKS}} - E^{\mathrm{KS}} = \langle R[\rho_{\mathrm{in}}(\mathbf{r})] C(\mathbf{r},\mathbf{r}') \{\rho_{\mathrm{out}}(\mathbf{r}') - \rho_{\mathrm{KS}}(\mathbf{r}')\}\rangle + O(\delta\rho^3), \tag{9}$$

$$E^{\mathrm{Harris}} - E^{\mathrm{KS}} = \langle R[\rho_{\mathrm{in}}(\mathbf{r})] C(\mathbf{r},\mathbf{r}') \{\rho_{\mathrm{in}}(\mathbf{r}') - \rho_{\mathrm{KS}}(\mathbf{r}')\}\rangle + O(\delta\rho^3), \tag{10}$$

where $C(\mathbf{r},\mathbf{r}')$ is given by

$$C(\mathbf{r},\mathbf{r}') = \frac{1}{2}\left(\frac{1}{|\mathbf{r}-\mathbf{r}'|} + \left. \frac{\delta v_{\mathrm{xc}}[\rho](\mathbf{r})}{\delta\rho(\mathbf{r}')} \right|_{\rho_{\mathrm{in}}} \right). \tag{11}$$

The difference between the HKS and the Harris functionals can be then easily estimated via Eqs. (9) and (10),

$$E^{\mathrm{HKS}}[\rho_{\mathrm{in}},\rho_{\mathrm{out}}] - E^{\mathrm{Harris}}[\rho_{\mathrm{in}},\rho_{\mathrm{out}}] = \langle R[\rho_{\mathrm{in}}(\mathbf{r})] C(\mathbf{r},\mathbf{r}') R[\rho_{\mathrm{in}}(\mathbf{r}')]\rangle + O(\delta\rho^3). \tag{12}$$

Based on Eqs. (9) and (10), we can define the corrected HKS (cHKS) and the corrected Harris (cHarris) functionals as the HKS and the Harris functionals with their own second-order corrections,

$$E^{\mathrm{cHKS}}[\rho_{\mathrm{in}},\rho_{\mathrm{out}}] = E^{\mathrm{HKS}}[\rho_{\mathrm{in}},\rho_{\mathrm{out}}] + \langle R[\rho_{\mathrm{in}}(\mathbf{r})] C(\mathbf{r},\mathbf{r}') \times \{\rho_{\mathrm{KS}}(\mathbf{r}') - \rho_{\mathrm{out}}(\mathbf{r}')\}\rangle, \tag{13}$$

$$E^{\mathrm{cHarris}}[\rho_{\mathrm{in}},\rho_{\mathrm{out}}] = E^{\mathrm{Harris}}[\rho_{\mathrm{in}},\rho_{\mathrm{out}}] + \langle R[\rho_{\mathrm{in}}(\mathbf{r})] C(\mathbf{r},\mathbf{r}') \times \{\rho_{\mathrm{KS}}(\mathbf{r}') - \rho_{\mathrm{in}}(\mathbf{r}')\}\rangle, \tag{14}$$

respectively. We note that the series expansion of the total energy in the SCM of Ullmo *et al.*[15] is essentially the cHarris functional,[18]

$$E^{\mathrm{SCM}} = E^{\mathrm{cHarris}}[\rho_{\mathrm{in}},\rho_{\mathrm{out}}]. \tag{15}$$

To further cancel the errors in the HKS and the Harris functionals, we proposed the following Zhou-Wang-λ (ZWλ) functional:[19]

$$E^{\mathrm{ZW}\lambda}[\rho_{\mathrm{in}},\rho_{\mathrm{out}}] = (1-\lambda) E^{\mathrm{HKS}}[\rho_{\mathrm{in}},\rho_{\mathrm{out}}] + \lambda E^{\mathrm{Harris}}[\rho_{\mathrm{in}},\rho_{\mathrm{out}}], \tag{16}$$

where λ is an interpolation parameter. A close inspection of Eqs. (9), (10), and (12) discloses the second-order error of the ZWλ functional,

$$E^{\mathrm{ZW}\lambda} - E^{\mathrm{KS}} = \langle R[\rho_{\mathrm{in}}(\mathbf{r})] C(\mathbf{r},\mathbf{r}') \{\rho_{\mathrm{out}}(\mathbf{r}') - \rho_{\mathrm{KS}}(\mathbf{r}')\}\rangle - \lambda \langle R[\rho_{\mathrm{in}}(\mathbf{r})] C(\mathbf{r},\mathbf{r}') R[\rho_{\mathrm{in}}(\mathbf{r}')]\rangle + O(\delta\rho^3). \tag{17}$$

The optimal λ that renders the right-hand side of the above equation vanish through second order can be evaluated via

$$\lambda = \frac{\langle R[\rho_{\mathrm{in}}(\mathbf{r})] C(\mathbf{r},\mathbf{r}') \{\rho_{\mathrm{out}}(\mathbf{r}') - \rho_{\mathrm{KS}}(\mathbf{r}')\}\rangle}{\langle R[\rho_{\mathrm{in}}(\mathbf{r})] C(\mathbf{r},\mathbf{r}') R[\rho_{\mathrm{in}}(\mathbf{r}')]\rangle} \doteq \frac{\langle R[\rho_{\mathrm{in}}(\mathbf{r})] C(\mathbf{r},\mathbf{r}') \{\rho_{\mathrm{out}}(\mathbf{r}') - \rho_{\mathrm{KS}}(\mathbf{r}')\}\rangle}{E^{\mathrm{HKS}} - E^{\mathrm{Harris}}}, \tag{18}$$

where the second equal sign is due to Eq. (12). Interestingly, the ZWλ functional reduces to the cHKS functional with the insertion of Eq. (18) into Eq. (16).

By subtracting the Roothaan energy,[27,28]

$$E^{\mathrm{R}}[\rho_{\mathrm{in}},\rho_{\mathrm{out}}]=\frac{1}{2}\left\langle\frac{R[\rho_{\mathrm{in}}(\mathbf{r})]R[\rho_{\mathrm{in}}(\mathbf{r}')]}{|\mathbf{r}-\mathbf{r}'|}\right\rangle, \tag{19}$$

from the HKS functional, we recently proposed the Wang-Zhou (WZ) functional,[20]

$$\begin{aligned}E^{\mathrm{WZ}}[\rho_{\mathrm{in}},\rho_{\mathrm{out}}]&=E^{\mathrm{HKS}}[\rho_{\mathrm{in}},\rho_{\mathrm{out}}]-E^{\mathrm{R}}[\rho_{\mathrm{in}},\rho_{\mathrm{out}}]\\&=\sum_i f_i\epsilon_i-E_{\mathrm{H}}[\rho_{\mathrm{in}}]+E_{\mathrm{xc}}[\rho_{\mathrm{out}}]\\&\quad-\langle\rho_{\mathrm{out}}(\mathbf{r})v_{\mathrm{xc}}[\rho_{\mathrm{in}}](\mathbf{r})\rangle.\end{aligned} \tag{20}$$

The WZ functional always produces a lower total energy than does the HKS functional since the Roothaan energy is always positive.[27,28] We also found that the WZ functional usually converges to E^{KS} from below;[20] however, whether it is a lower bound to E^{KS} remains to be proven. A linear mixing of the HKS and the WZ functionals leads to the Wang-Zhou-α (WZα) functional,[20]

$$\begin{aligned}E^{\mathrm{WZ}\alpha}[\rho_{\mathrm{in}},\rho_{\mathrm{out}}]&=(1-\alpha)E^{\mathrm{HKS}}[\rho_{\mathrm{in}},\rho_{\mathrm{out}}]+\alpha E^{\mathrm{WZ}}[\rho_{\mathrm{in}},\rho_{\mathrm{out}}]\\&=E^{\mathrm{HKS}}[\rho_{\mathrm{in}},\rho_{\mathrm{out}}]-\alpha E^{\mathrm{R}}[\rho_{\mathrm{in}},\rho_{\mathrm{out}}],\end{aligned} \tag{21}$$

with the mixing parameter α. From Eqs. (9) and (21), we can estimate the second-order error of the WZα functional,

$$\begin{aligned}E^{\mathrm{WZ}\alpha}-E^{\mathrm{KS}}&=\langle R[\rho_{\mathrm{in}}(\mathbf{r})]C(\mathbf{r},\mathbf{r}')\{\rho_{\mathrm{out}}(\mathbf{r}')-\rho_{\mathrm{KS}}(\mathbf{r}')\}\rangle\\&\quad-\alpha E^{\mathrm{R}}[\rho_{\mathrm{in}},\rho_{\mathrm{out}}]+O(\delta\rho^3).\end{aligned} \tag{22}$$

The optimal α value that renders the second-order error in $E^{\mathrm{WZ}\alpha}$ vanish is then given by

$$\alpha=\frac{\langle R[\rho_{\mathrm{in}}(\mathbf{r})]C(\mathbf{r},\mathbf{r}')\{\rho_{\mathrm{out}}(\mathbf{r}')-\rho_{\mathrm{KS}}(\mathbf{r}')\}\rangle}{E^{R}[\rho_{\mathrm{in}},\rho_{\mathrm{out}}]}. \tag{23}$$

Again, the WZα functional reduces to the cHKS functional with the optimal α defined above. Thus, we have the following identity:

$$E^{\mathrm{ZW}\lambda}[\rho_{\mathrm{in}},\rho_{\mathrm{out}}]=E^{\mathrm{WZ}\alpha}[\rho_{\mathrm{in}},\rho_{\mathrm{out}}]=E^{\mathrm{cHKS}}[\rho_{\mathrm{in}},\rho_{\mathrm{out}}], \tag{24}$$

for the optimal values of λ and α defined in Eqs. (18) and (23).

Although the incorporation of the second-order corrections improves the accuracy of the total energy evaluation, a practical difficulty is the lack of the *a priori* unknown exact KS density $\rho_{\mathrm{KS}}(\mathbf{r})$, for which a good approximation must be adopted. In the work of Ullmo *et al.*, a scheme was devised to obtain $\rho_{\mathrm{KS}}(\mathbf{r})$ by invoking an auxiliary system in the framework of OF-DFT.[15] However, we found that their scheme suffers from several drawbacks.[18] Benoit *et al.* proposed another perturbative scheme to approximate $\rho_{\mathrm{KS}}(\mathbf{r})$, but the computation of the functional derivative of the XC potential, $\delta v_{\mathrm{xc}}[\rho](\mathbf{r})/\delta\rho_{\mathrm{in}}(\mathbf{r}')$, is quite involved and expensive for some sophisticated XC functionals.[29,30]

On the other hand, high-quality density mixing schemes, such as the residual minimization method, direct inverse in the iterative space,[4,5] are quite robust for iterative KS-DFT calculations. At the ith iteration, a high-quality density mixing scheme [see Eq. (4)] is able to produce accurate input density for the next iteration, $\rho_{\mathrm{in}}^{i+1}(\mathbf{r})$, which is usually much better than the current-iteration input and output densities. Consequently, the optimal input density $\rho_{\mathrm{in}}^{i+1}(\mathbf{r})$ from such high-quality density mixing schemes can then be directly utilized to approximate $\rho_{\mathrm{KS}}(\mathbf{r})$ with very little extra computational and coding effort. Our previous work has demonstrated that this simple approach produces accurate second-order correction for the Harris functional.[18] In this work, we further generalize this method to the evaluation of the cHKS functional. As will be shown later, the amount of improvement that can be achieved by the cHKS and the cHarris functionals upon the widely used HKS and Harris functionals depend strongly on the quality of $\rho_{\mathrm{in}}^{i+1}(\mathbf{r})$.

Finally, we need to compute the functional derivative of the XC potential, $\delta v_{\mathrm{xc}}[\rho](\mathbf{r})/\delta\rho(\mathbf{r}')$, in the evaluation of $C(\mathbf{r},\mathbf{r}')$ in Eq. (11). To avoid the above mentioned difficulty in its direct numerical evaluation, we adopt the following finite-difference approximation:[18]

$$\begin{aligned}&\left\langle R[\rho_{\mathrm{in}}(\mathbf{r})]\ \frac{\delta v_{\mathrm{xc}}[\rho](\mathbf{r}')}{\delta\rho(\mathbf{r})}\bigg|_{\rho_{\mathrm{in}}}\right\rangle\\&\quad\approx v_{\mathrm{xc}}[\rho_{\mathrm{out}}](\mathbf{r}')-v_{\mathrm{xc}}[\rho_{\mathrm{in}}](\mathbf{r}'),\end{aligned} \tag{25}$$

which only introduces numerical errors higher than second order.

III. NUMERICAL RESULTS AND DISCUSSION

We test our new schemes in KS-DFT calculations on the following systems: the metallic Al–Si binary alloy, the cubic diamond (CD) Si vacancy and (100) surface. A cubic face-centered-cubic supercell containing 32 atomic sites is used for the Al–Si alloy, in which five Si atoms are put at randomly selected atomic sites and 27 Al atoms occupy the remaining sites. This $Al_{27}Si_5$ system approximately corresponds to an Al-xSi alloy with Si doping rate $x\approx 15\%$. A $2\times2\times2$ supercell containing 63 atoms and one vacancy is used for the CD Si vacancy. The CD Si (100) surface contains a five-layer slab with two atoms per layer and the vacuum has the same dimension as the slab. The local density approximation[31] (LDA) is used in all DFT calculations.

The initial density for KS-DFT calculations is obtained from OF-DFT calculations using the Wang-Govind-Carter KEDF,[32] which involves three parameters α, β, and γ. We set the values of $\{\alpha,\beta\}_\gamma$ to be $\left\{\frac{5}{6}\pm\frac{\sqrt{5}}{6}\right\}_{2.7}$ for the metallic Al–Si alloy and $\left\{\frac{5}{6}\pm\frac{\sqrt{5}}{6}\right\}_{3.6}$ for the CD Si vacancy and surface. The two different sets of parameters used here are found to be optimal for metallic and semiconducting systems, respectively.[32,33] The Goodwin-Needs-Heine LPS is used for Al,[34] while the LPS derived from a bulk environment[22] are employed for Si. More computational details of OF-DFT calculations are given in Refs. 19 and 20.

A modified ABINIT code[35] is used to run KS-DFT calculations, in which the standard Troullier-Martins NLPS (Ref. 36) is used. The kinetic energy cutoff for the plane-wave basis set is chosen to be 760 eV for all DFT calculations. For the CD Si vacancy, we find that it is adequate to only employ the Γ point for the Brillouin-zone (BZ) sampling.[37] For the CD Si (100) surface, a $6\times6\times1$ Monkhorst-Pack grid[38] with 28 irreducible $\mathbf{k}$ points is used for the BZ sampling.

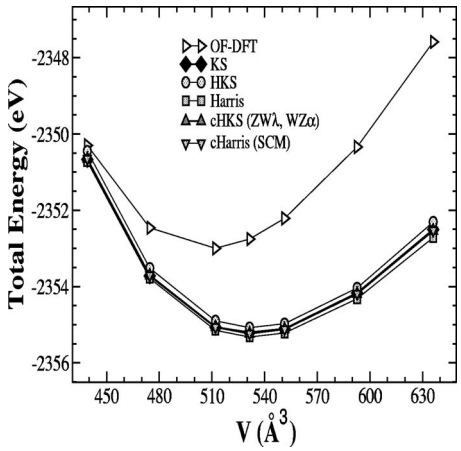

FIG. 1. LDA total energy (in eV) vs cell volume (in $Å^3$) for the $Al_{27}Si_5$ alloy. The results from OF-DFT (triangle right), one-iteration OO-DFT, and the self-consistent KS-DFT (solid diamond) are compared. In OO-DFT, we use the HKS (circle), the Harris (square), the cHKS (triangle up), and the cHarris (triangle down) functionals for the total energy evaluation. The cHKS, the cHarris, and the converged KS total energies overlap one another.

At the end of the first iteration of a KS-DFT calculation, the following Kerker's formula[39] (diagonal in reciprocal space) is used for the preconditioning matrix **G** in Eq. (4) for the reciprocal space wave vector q:

$$\mathbf{G}(q) = A\frac{q^2}{q^2 + q_0^2}, \tag{26}$$

where $A=0.8$ and $q_0=1.5$ $Å^{-1}$.[4] After the first iteration, Pulay's scheme[5] is employed for density mixing in subsequent iterations of the KS-DFT calculation.

Figure 1 depicts the total energies of the Al–Si alloy at different cell volumes obtained from OF-DFT, fully converged KS-DFT, and one-iteration OO-DFT calculations. OF-DFT leads to significant errors and only qualitatively reproduces the KS-DFT results. The overestimation of the total energy by OF-DFT becomes more severe when the cell volume increases. In OO-DFT, we compare the results from the HKS, the Harris, the cHKS, and the cHarris functionals. At different cell volumes, the HKS and the Harris functionals slightly overestimate and underestimate the total energies, respectively. Both the HKS and the Harris functionals adequately reduce the errors from OF-DFT and yield good total energies but still with increased numerical errors for bigger cell volumes. On the other hand, it is amazing to see that both the cHKS and the cHarris functionals almost exactly reproduce the total energies of fully converged KS-DFT with just one iteration.

In Fig. 2, the convergence behaviors of the cHKS and the cHarris functionals are compared with those of the HKS and the Harris functionals. Being consistent with our previous assessment in Eq. (24), Fig. 2 clearly shows that the ZWλ and the WZα functionals are essentially the cHKS functional. For the CD Si vacancy [Fig. 2(a)], the Harris functional is usually slightly more accurate than the HKS functional. In contrast, the convergence pattern of the cHKS and the cHarris functionals are almost identical, which implies that the contribution of the second-order correction in the cHKS functional is a bit larger than that in the cHarris functional. Moreover, both the cHKS and the cHarris functionals are usually more accurate than the HKS and the Harris functionals by one to two orders of magnitudes except at the second and fifth iterations. This is not surprising because the Pulay density mixing method[5] occasionally generates less accurate input density $\rho_{\text{in}}^{i+1}(\mathbf{r})$, which delivers little improvement. Of course, any future developments in devising better, faster, more stable generally applicable density mixing schemes will certainly enhance the performance of the cHKS and the cHarris functionals for this kind of difficult cases. Before such superpowerful density mixing schemes become available, we have no choice but to rely on the Pulay density mixing method,[5] which is widely regarded as the present most robust general-purpose scheme of generating high-quality initial guesses of density, orbitals, and wave function for the next iteration in a self-consistent field calculation.[4] Also notice that the errors in the cHKS and the cHarris func-

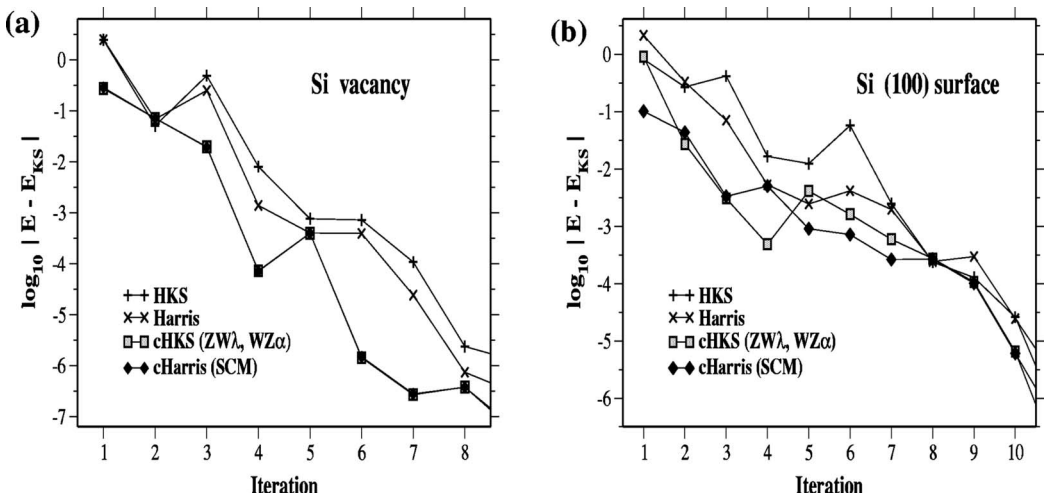

FIG. 2. Convergence of total energies (in eV) evaluated from the HKS (pluses), the Harris (crosses), the cHKS (opaque squares), and the cHarris (solid diamonds) functionals during the self-consistent iterations of KS-DFT calculations for (a) the CD Si vacancy and (b) the CD Si (100) surface. The cHKS functional also represents the ZWλ and the WZα functionals and the cHarris functional yields identical result to the SCM. In (a), the cHKS and the cHarris curves overlap each other.

tionals are within 1 meV at the fourth iteration, whereas three more iterations are needed for the HKS and the Harris functionals to reach the similar accuracy.

For the CD Si (100) surface, the convergence patterns of the four total energy functionals are more complicated as reflected by the fluctuations in Fig. 2(b). Nonetheless, we again observe that the cHKS and the cHarris functionals are usually better than the HKS and the Harris functionals by one or two orders of magnitude. However, the total energies from the cHKS and the cHarris functionals evince slightly different accuracies. The errors of the cHKS and the cHarris functionals are below 1 meV at the fourth iteration and after the fifth iteration, respectively. Interestingly, the cHarris functional converges faster and more smoothly than does the cHKS functional.

IV. CONCLUSIONS

In conclusion, two new functionals, i.e., the cHKS and the cHarris functionals, which include the second-order corrections, are proposed for the total electronic energy evaluation in iterative KS-DFT calculations. It is further realized that with the optimal mixing parameters, λ and α, defined in this work, the recently proposed ZWλ and WZα functionals are essentially the same as the cHKS functional. A practical scheme is then designed for the evaluation of the second-order corrections in the cHKS and the cHarris functionals. The key point in our new scheme lies in that the optimal input density from a robust density mixing scheme is used to approximate the exact KS density. For the metallic alloy system, the cHKS and the cHarris functionals further reduce the errors in the HKS and the Harris functionals, and both new functionals almost exactly reproduce the converged KS total energies with only one iteration of OO-DFT calculation. In iterative KS-DFT calculations for highly inhomogeneous surface and vacancy systems, the cHKS and the cHarris functionals usually yield more accurate total energies than the widely used HKS and Harris functionals by one to two orders of magnitude. This approach constitutes a practical generalization of the SCM and the OO-DFT methods and can also be employed in other iterative *ab initio* quantum chemistry methods.

ACKNOWLEDGMENTS

Financial support for this project was provided by a grant from the Natural Sciences and Engineering Research Council (NSERC) of Canada.

[1] R. G. Parr and W. Yang, *Density-Functional Theory of Atoms and Molecules* (Clarendon, New York, 1989); R. M. Dreizler and E. K. U. Gross, *Density Functional Theory: An Approach to the Quantum Many-Body Problem* (Springer-Verlag, Berlin, 1990).
[2] P. Hohenberg and W. Kohn, Phys. Rev. **136**, B864 (1964).
[3] W. Kohn and L. J. Sham, Phys. Rev. **140**, A1133 (1965).
[4] G. Kresse and J. Furthmüller, Comput. Mater. Sci. **6**, 15 (1996).
[5] P. Pulay, Chem. Phys. Lett. **73**, 393 (1980).
[6] D. Vanderbilt and S. G. Louie, Phys. Rev. B **30**, 6118 (1984); G. P. Srivastava, J. Phys. A **17**, L317 (1984); D. D. Johnson, Phys. Rev. B **38**, 12807 (1988).
[7] J. R. Chelikowsky and S. G. Louie, Phys. Rev. B **29**, 3470 (1984).
[8] S. Goedecker, Rev. Mod. Phys. **71**, 1085 (1999).
[9] A. Stathopoulos, S. Öğüt, Y. Saad, J. Chelikowsky, and H. Kim, Comput. Sci. Eng. **2**, 19 (2000).
[10] F. Shimojo, R. K. Kalia, A. Nakano, and P. Vashishta, Comput. Phys. Commun. **140**, 303 (2001).
[11] L. H. Thomas, Proc. Cambridge Philos. Soc. **23**, 542 (1927); E. Fermi, Rend. Accad. Naz. Lincei **6**, 602 (1927); Z. Phys. **48**, 73 (1928).
[12] W. H. Press, B. P. Flannery, S. A. Teukolsky, and W. T. Vetterling, *Numerical Recipes in Fortran* (Cambridge University Press, Cambridge, 1992).
[13] Y. A. Wang and E. A. Carter, in *Theoretical Methods in Condensed Phase Chemistry*, edited by S. D. Schwartz (Kluwer, Dordrecht, 2000), p. 117.
[14] N. Choly and E. Kaxiras, Solid State Commun. **121**, 281 (2002).
[15] D. Ullmo, T. Nagano, S. Tomsovic, and H. U. Baranger, Phys. Rev. B **63**, 125339 (2001).
[16] D. Ullmo, T. Nagano, and H. U. Baranger, Phys. Rev. B **64**, 245324 (2001); D. Ullmo, H. Jiang, W. Yang, and H. U. Baranger, *ibid.* **70**, 205309 (2004); H. Jiang, D. Ullmo, W. Yang, and H. U. Baranger, *ibid.* **71**, 085313 (2005); D. Ullmo, T. Nagano, and S. Tomsovic, Phys. Rev. Lett. **90**, 176801 (2003).
[17] C. Yannouleas and U. Landman, Chem. Phys. Lett. **210**, 437 (1993); Chem. Phys. Lett. **217**, 175 (1994); Phys. Rev. B **48**, 8376 (1993); C. Yannouleas, E. N. Bogachek, and U. Landman, *ibid.* **57**, 4872 (1998); C. Yannouleas and U. Landman, J. Phys. Chem. B **101**, 5780 (1997).
[18] B. Zhou and Y. A. Wang, J. Chem. Phys. **127**, 064101 (2007).
[19] B. Zhou and Y. A. Wang, J. Chem. Phys. **124**, 081107 (2006).
[20] B. Zhou and Y. A. Wang, Int. J. Quantum Chem. **107**, 2995 (2007).
[21] W. E. Pickett, Comput. Phys. Rep. **9**, 115 (1989).
[22] B. Zhou, Y. A. Wang, and E. A. Carter, Phys. Rev. B **69**, 125109 (2004).
[23] J. Harris, Phys. Rev. B **31**, 1770 (1985).
[24] M. W. Finnis, J. Phys.: Condens. Matter **2**, 331 (1990).
[25] I. J. Robertson and B. Farid, Phys. Rev. Lett. **66**, 3265 (1991); E. Zaremba, J. Phys.: Condens. Matter **2**, 2479 (1990).
[26] H. M. Polatoglou and M. Methfessel, Phys. Rev. B **37**, 10403 (1988); A. J. Read and R. J. Needs, J. Phys.: Condens. Matter **1**, 7565 (1989).
[27] C. C. J. Roothaan, Rev. Mod. Phys. **23**, 69 (1951), Appendix I.
[28] B. I. Dunlap, J. W. D. Connolly, and J. R. Sabin, J. Chem. Phys. **71**, 3396 (1979).
[29] D. M. Benoit, D. Sebastiani, and M. Parrinello, Phys. Rev. Lett. **87**, 226401 (2001).
[30] W. Zhu and S. B. Trickey, Int. J. Quantum Chem. **100**, 245 (2004).
[31] J. P. Perdew and A. Zunger, Phys. Rev. B **23**, 5048 (1981).
[32] Y. A. Wang, N. Govind, and E. A. Carter, Phys. Rev. B **60**, 16350 (1999); **64**, 089903(E) (2001).
[33] B. Zhou, V. L. Lignères, and E. A. Carter, J. Chem. Phys. **122**, 044103 (2005).
[34] L. Goodwin, R. J. Needs, and V. Heine, J. Phys.: Condens. Matter **2**, 351 (1990).
[35] X. Gonze, J.-M. Beuken, R. Caracas, F. Detraux, M. Fuchs, G.-M. Rignanese, L. Sindic, M. Verstraete, G. Zerah, F. Jollet, M. Torrent, A. Roy, M. Mikami, P. Ghosez, J.-Y. Raty, and D. C. Allan, Comput. Mater. Sci. **25**, 478 (2002).
[36] N. Troullier and J. L. Martins, Phys. Rev. B **43**, 1993 (1991).
[37] N. W. Ashcroft and N. D. Mermin, *Solid State Physics* (Saunders, Orlando, 1976).
[38] H. J. Monkhorst and J. D. Pack, Phys. Rev. B **13**, 5188 (1976).
[39] G. P. Kerker, Phys. Rev. B **23**, 3082 (1981).